

ESTIMATION OF PERMANENT DEFORMATION IN ASPHALT CONCRETE LAYERS DUE TO REPEATED TRAFFIC LOADING

D. B. McLean, E. W. Brooker and Associates, Edmonton, Alberta, Canada; and
C. L. Monismith, Institute of Transportation and Traffic Engineering,
University of California, Berkeley

Methodology to permit estimation of permanent deformation (rutting) in pavement structures from repeated load triaxial compression and creep tests is discussed. Techniques to estimate the distortion characteristics of asphalt concrete and the use of these data together with linear viscoelastic theory to predict rutting in asphalt-bound layers of pavement structures are concentrated on. Although there is little field data to demonstrate the development of rutting with load repetitions under controlled conditions, Hofstra and Klomp have presented such data from test track studies. The use of the repeated load test data together with elastic theory gives the same form of relation of rut depth versus load applications measured by Hofstra and Klomp suggesting that the procedure has potential to examine this facet of design. When used to study the influence of various parameters on pavement response, this approach led to the following: Subgrade stiffness appears to have little influence on the accumulation of rutting in the asphalt-bound layer, at least for the stiffness range examined; asphalt concrete stiffness exerts significant influence on rutting in the asphalt-bound layer; and rut depth in the asphalt layer is independent of layer thickness for the range examined. The procedure in which the creep test was used to estimate rutting provided estimates that were very small. Moreover, the shape of the rut depth versus the application relation determined by using this methodology did not resemble the form reported by Hofstra and Klomp. These observations require that a careful evaluation be made to ascertain the reasons for these apparent discrepancies.

•IT is possible to analyze the pavement structure within a reasonable framework to ascertain effects of load and environmental factors on pavement response. After comparing the results of such analyses with the limiting response characteristics of the pavement materials or a predetermined condition (e.g., limiting rut depth or surface friction coefficient), pavement performance can be judged. Then, appropriate action can be taken to minimize specific distress modes.

This paper is concerned with the distortion mode of distress and the permanent deformation (rutting) that results from repeated traffic loading. Renewed interest has developed in this phase of the design process as evidenced by the recent work of Heukelom and Klomp (1); Barksdale (2); Romain (3); Elliot (4); Elliot, Moavenzadeh, and Findakly (5); and Hofstra and Klomp (6). Figure 1 shows a subsystem of the pavement design system that permits consideration of the distortion mode. This paper concentrates primarily on structural analysis estimating distortion characteristics, and distortion prediction.

LABORATORY TEST PROGRAM

The measurement of the permanent deformation characteristics of asphalt-bound materials (and other structural pavement materials) requires that the materials be

Figure 1. Distortion subsystem.

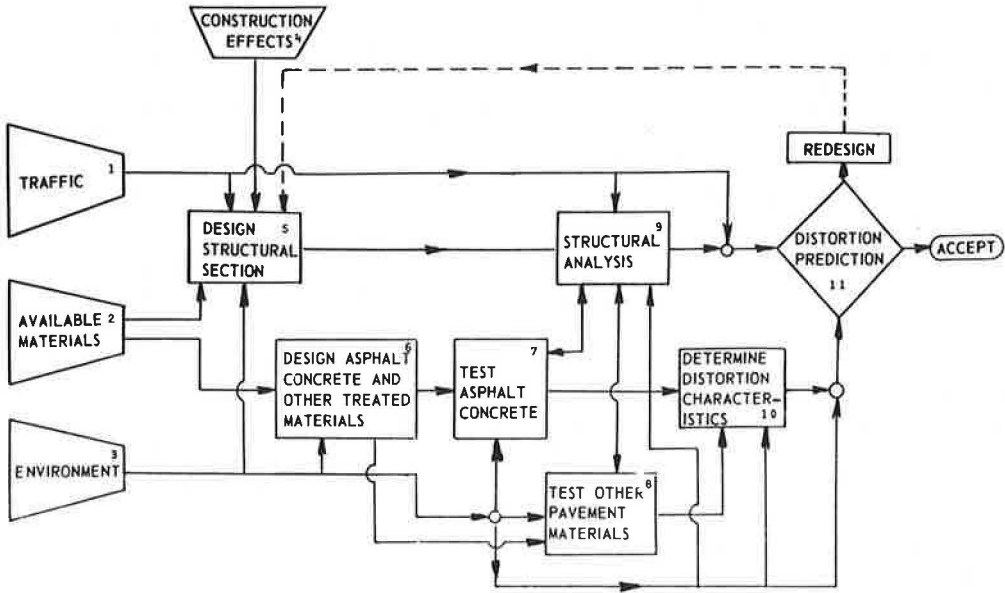
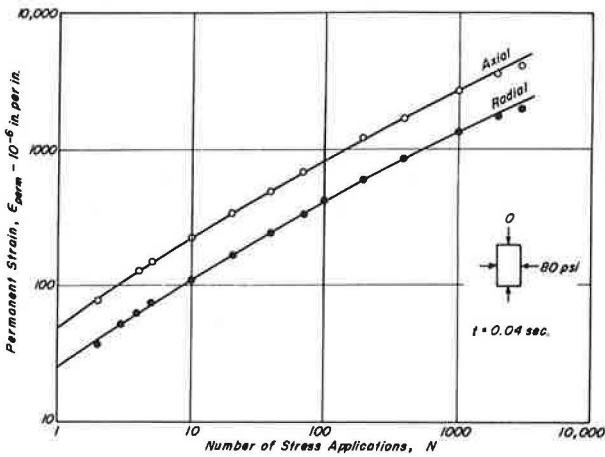


Figure 2. Extension test results, 67 F.



tested under representative service conditions, which include realistic stress states, times of loading, and temperatures.

McLean (7) prepared a detailed analysis of loading and temperature conditions. Test conditions that resulted from this analysis are summarized briefly in the Appendix. Loading times had the same dependency as those suggested by Barksdale (2).

To simulate different loading conditions, the repeated load triaxial-compression equipment developed by Dehlen (8) was used. Use of this equipment permitted independent application of axial and radial stresses in repeated loading. The Appendix contains a brief description of the equipment and procedures used to test asphalt concrete specimens in repeated loading.

Creep testing also was performed on asphalt concrete to be used in the predictive procedure, VESYS II, developed by the Federal Highway Administration (FHWA) to estimate the accumulation of permanent deformation (9). This test procedure also is described in the Appendix.

Test Results

Results of repeated load tests over a range in temperatures are shown in Figures 2, 3, and 4. Each figure shows a different type of test and associated terminology. The following are stress states and their locations for thick, asphalt-bound layers:

1. Extension—near the surface,
2. Compression—center of layer, and
3. Tension—near the lower boundary.

Interestingly, the slopes of the strain versus number of stress application curves were essentially the same regardless of the type of test used to induce the permanent deformation.

The strain data shown in Figures 2, 3, and 4 were corrected for volume strains according to the following relation:

$$\epsilon_{\text{corr}}^p = \epsilon_{\text{measured}}^p - \frac{1}{3} [\Delta V/V] \quad (1)$$

where $\Delta V/V$ = volume strain.

Axial creep compliance from extension tests over a range of temperatures is shown in Figure 5. Rather than use strain as in Figures 2, 3, and 4, a creep compliance was determined from the following:

$$\Psi_{\epsilon}(t) = \frac{\epsilon_A(t)}{\sigma_A - \sigma_R} \quad (2)$$

where

- $\Psi_{\epsilon}(t)$ = axial creep compliance,
- $\epsilon_A(t)$ = axial strain,
- σ_A = applied axial stress, and
- σ_R = radial stress.

Compression tests also were conducted; results were of the same form as shown in Figure 5.

Analyses

The technique used to estimate rutting fitted to data similar to the data shown in Figures 2, 3, and 4 the following third order polynomial by using a least squares procedure:

$$\log \epsilon^p = C_0 + C_1 \log N - C_2 (\log N)^2 + C_3 (\log N)^3 \quad (3)$$

Figure 3. Compression test results, 85 F.

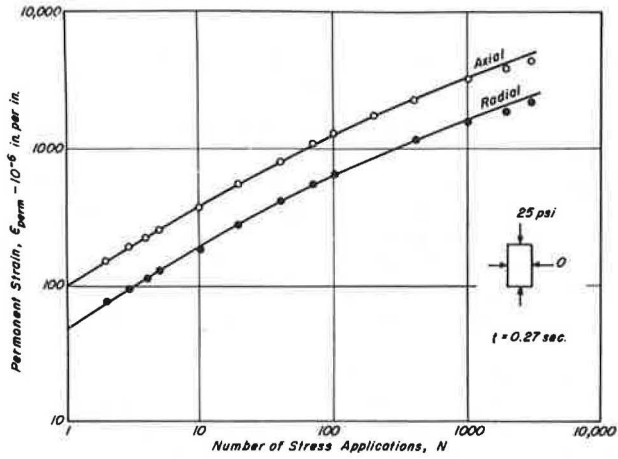


Figure 4. Tension test results, 100 F.

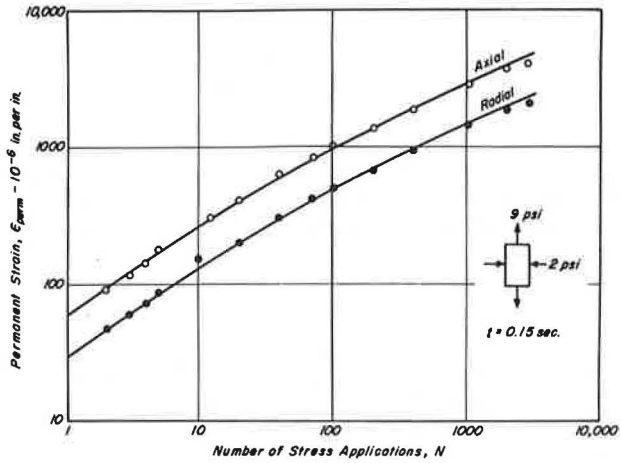
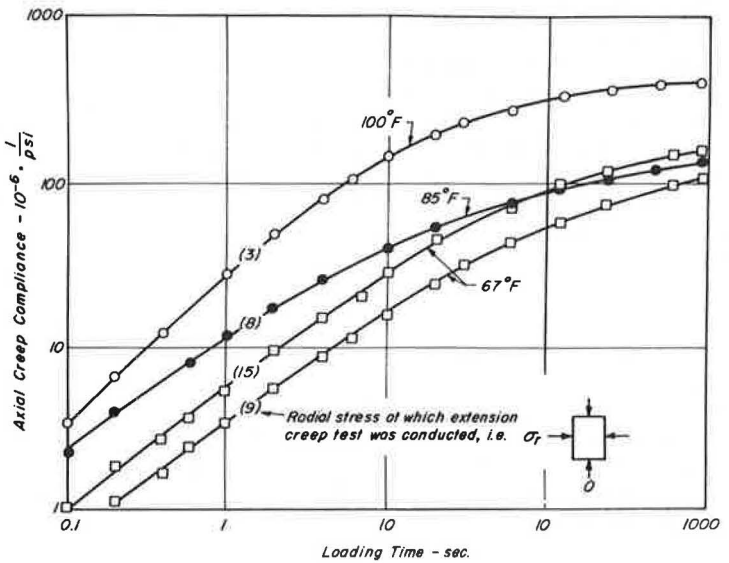


Figure 5. Axial creep compliance from extension tests.



where

ϵ^p = plastic strain (corrected for volume change) and
 N = number of stress applications.

The influences of stress state, time of loading, and temperature are reflected in the coefficients C_0 , C_1 , C_2 , and C_3 .

In developing the least squares relationships it was found that the polynomials were very sensitive to the first and last data points. To reduce the sensitivity, the first data point ($N = 1$) was eliminated because seating errors tended to influence the initial readings. Because the majority of tests were stopped at less than 10,000 repetitions, the data were linearly extrapolated to $N = 10^5$ to control the fit at large numbers of repetitions; this must be considered a suitable technique until additional data become available.

For this mix, analyses of the data do not indicate any apparent trends with temperature, stress level, stress direction, or elastic strain for the coefficients C_1 , C_2 , and C_3 . Unfortunately, however, no analyses were performed to define the independence of the coefficients or their interdependence. The results of the analyses are as follows:

| <u>Coefficient</u> | <u>Mean</u> | <u>Standard Deviation</u> |
|--------------------|-------------|---------------------------|
| C_1 | 0.85 | 0.14 |
| C_2 | 0.013 | 0.006 |
| C_3 | -0.14 | 0.06 |

The coefficient C_0 (in this case, the logarithm of permanent deformation resulting from initial load application) appeared to depend on a number of factors including stress, strain, and temperature. To combine the influence of stress and strain on C_0 at a particular temperature the following relationship was developed:

$$\epsilon_1^p = K(\sigma_d \cdot \epsilon_e)^n \quad (4)$$

where

$\epsilon_1^p = 10^{C_0}$, permanent strain at first load repetition;
 $\sigma_d = \sigma_A - \sigma_R$, stress difference in triaxial compression;
 ϵ_e = elastic strain; and
 K, n = experimentally determined coefficients.

Figure 6 shows data and regression lines that conform to Eq. 4 for axial and radial deformations including both extension and compression results. This form permits making an estimate of permanent deformation in pavement structure that results from an applied load at the surface.

Data from the repeated load tests can be examined in other ways. To illustrate the variations in total, elastic, and permanent strain, data for the specimen whose permanent strain characteristics are shown in Figure 4 are plotted in Figure 7. The permanent strain per load application relationship shown in this figure was obtained by differentiating the curve of the form of Eq. 3, which had been fitted to the data of Figure 4. In Figure 7, after about 100 stress repetitions, the permanent strain per cycle was small.

ANALYSIS OF PAVEMENT STRUCTURES

To estimate permanent deformation from repetitive traffic loading, Heukelom and Klomp (1), Barksdale (2), and Romain (3) suggested the elastic layer theory to compute stresses and strains. They also suggested using these values to estimate permanent deformations from appropriate constitutive relationships. Viscoelastic layer theory, together with creep data incorporated in an analysis such as that developed by Elliott et al. (4) and included in the FHWA program VESYS II, can be used also to estimate permanent deformation.

Figure 6. Repeated load triaxial compression test results.

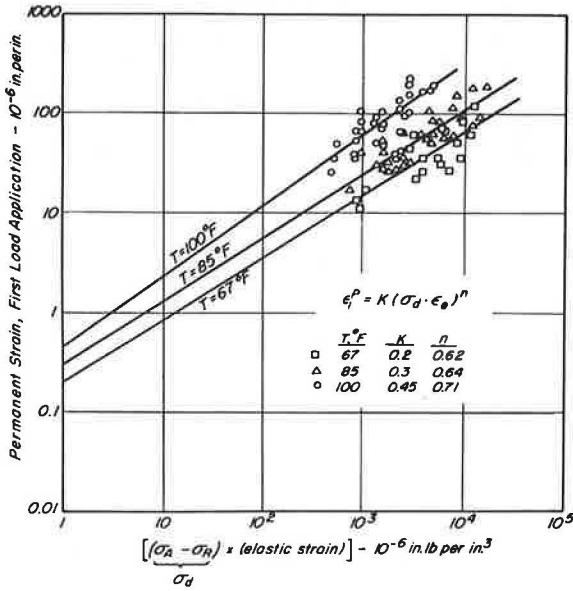


Figure 7. Variations in total, elastic, and permanent strain, tension test, 100 F.

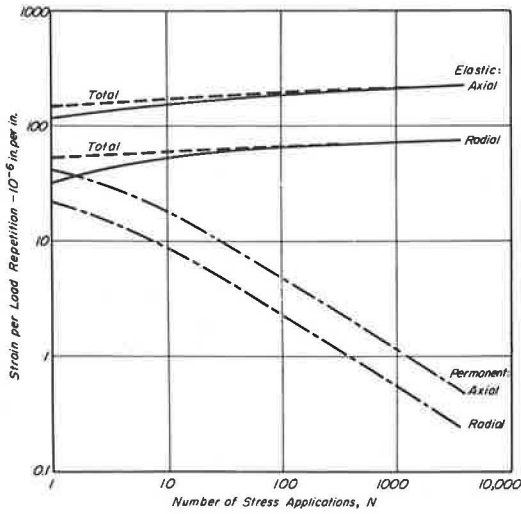
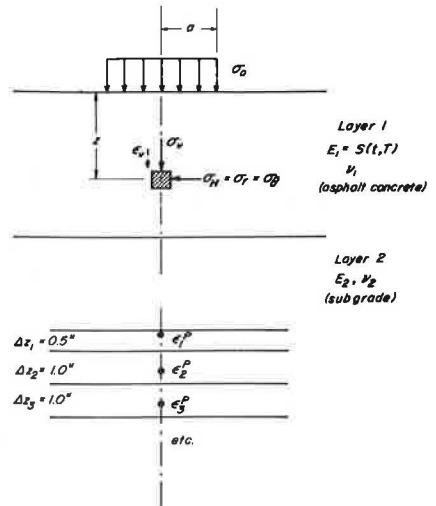


Figure 8. Schematic of pavement system used to estimate permanent deformation.



Elastic Analysis

In this procedure the elastic layer program CHEV 5L and the relationships represented by Eqs. 3 and 4 were used. For simplicity, the computations were done for a 2-layer system (asphalt concrete directly on subgrade) and for a load applied to a single circular area. The procedure suggested by Barksdale (2), where the layer under consideration is subdivided into a series of layers, was followed. Computations were performed at 1-in. (2.5-cm) intervals throughout the depth of the upper layer and at the boundaries—all on the axis of the loaded area. Also, the upper layer was assumed to have a constant stiffness modulus.

To permit the use of Eqs. 3 and 4 it was first necessary to compute σ_d and ϵ_s of Eq. 4. These were determined, as shown in Figure 8, with the aid of the computer program by assuming

$$\sigma_d = \sigma_v - \sigma_h \quad (5)$$

and

$$\epsilon_s = \epsilon_v \quad (6)$$

where

σ_v = vertical stress,

σ_h = horizontal stress (radial and tangential stresses are equal for the condition analyzed), and

ϵ_v = vertical strain.

These values were then used for a number of load repetitions to compute permanent strains, which, in turn, permitted permanent deformation in the layer to be obtained from the relation

$$\delta^p = \sum_{i=1}^n (\epsilon_i^p \Delta z_i) \quad (7)$$

where

δ^p = rut depth or permanent deformation in the upper (asphalt-bound) layer and

ϵ_i^p = permanent strain in subdivided layer (Fig. 8).

A series of pavement systems were studied by this procedure to ascertain the influence of various factors on the accumulation of permanent deformation.

To ensure that the procedure under investigation was reasonable, rut depth versus number of load repetitions obtained under controlled conditions by Hofstra and Klomp (6) was included for comparison. Their data were obtained by subjecting an 8-in. (20-cm) layer of asphalt concrete resting directly on a subgrade to a 1,500-lb (6 700-N) wheel load with a contact pressure of 70 psi (485 kPa) in a laboratory test track. About 200,000 load repetitions were applied at a temperature of 86 F (30 C).

Computations were made by using the procedure described above with the same asphalt concrete stiffness as that reported by Hofstra and Klomp, 155,000 psi (1 070 MPa), and the same subgrade modulus, 28,000 psi (193 MPa). The mix tested by Hofstra and Klomp contained a 40-50 penetration asphalt cement and was considered an overasphalted mix because it had less than 2 percent air voids. The mix whose data were reported in the previous section contained an 85-100 penetration asphalt cement and had a void content in the range of 4 to 6 percent. At the 86 F (30 C) temperature and time of loading reported by Hofstra and Klomp, this mix exhibited a stiffness of 2.5×10^5 psi (17 200 MPa). In a comparison of the results, the form of the load-deformation relationship is more important than the absolute magnitude of the deformations.

Table 1 contains the parameters used in the computations for 5 cases. Results of these computations are shown in Figure 9 for comparison with the Hofstra and Klomp

Table 1. Data used for sensitivity studies of permanent deformation estimation.

| Condition | Coefficients of Equation 4 | | Coefficients of Equation 3 | | |
|-----------------------------------|----------------------------|------|----------------------------|----------------|----------------|
| | K | n | C ₁ | C ₂ | C ₃ |
| 1. Mean | 0.37 | 0.66 | 0.85 | -0.14 | 0.013 |
| 2. K _{mean} + 10 percent | 0.41 | 0.66 | 0.85 | -0.14 | 0.013 |
| 3. K _{mean} - 10 percent | 0.37 | 0.72 | 0.85 | -0.14 | 0.013 |
| 4. Max. of range | 0.37 | 0.66 | 1.23 | -0.33 | 0.032 |
| 5. Min. of range | 0.37 | 0.66 | 0.62 | -0.035 | 0.0027 |

Figure 9. Rut depths, computed data versus Hofstra and Klomp data.

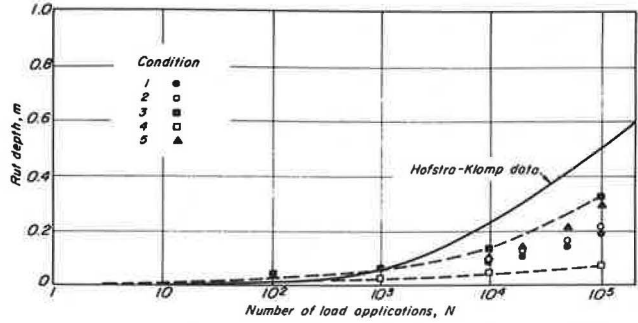
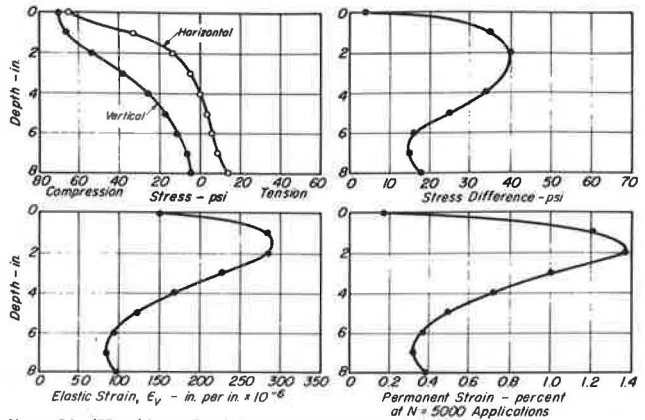
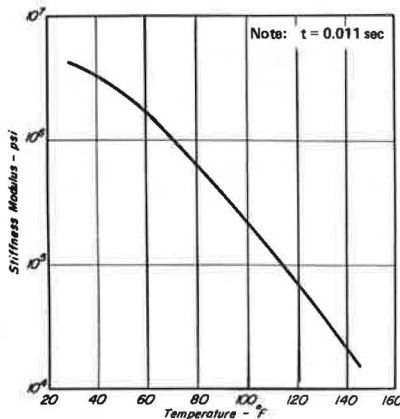


Figure 10. Stress and strain distributions.



Note: 8-in. (20-cm) layer of asphalt concrete pavement subjected to 1,500-lb (6 700-N) wheel load with a contact pressure of 70 psi (485 kPa)

Figure 11. Stiffness versus temperature.



data. Although the mixtures were different, the shapes of the curves were similar, indicating the potential of this procedure.

Figure 10 shows the distribution of elastic stresses and strains and permanent strains with depth for the mean condition given in Table 1 (at $N = 5,000$ stress applications for permanent strain). In Figure 10 the distribution of permanent strain is similar in shape to the distributions of stress difference and elastic vertical strain. Hofstra and Klomp observed that the distribution of permanent strain was fairly uniformly distributed in the layers of each section of the laboratory test track pavements. A number of factors might contribute to this difference. For example, time of loading was assumed constant with depth (constant stiffness modulus). The analyses of Barksdale (2) and McLean (7) indicated an increase in loading time with depth, which, in turn, reduced the stiffness. As will be seen, this could influence the distribution of permanent strain.

To examine the influence of material characteristics, temperature, and pavement thickness, a series of solutions was developed by using this procedure. Two subgrade stiffnesses—5,000 psi (34 500 kPa) and 10,000 psi (69 000 kPa)—were used. The stiffness versus temperature relationship shown in Figure 11 was used for the asphalt concrete layer. [The time of loading of 0.011 sec corresponds to that associated with the vertical stress at intermediate depth in a 12-in. (30.5-cm) layer for a vehicle speed of 60 mph (27 m/s) (7).] The other factors are given in Table 2. Mean values for the coefficients C_1 , C_2 , and C_3 as given in Table 1 were used. Computations were made for a 4,500-lb (20 000-N) wheel load with a contact pressure of 80 psi (550 kPa).

The influence of the stiffness of the asphalt concrete on rut depth is shown in Figure 12. Reducing the stiffness by a factor of 2 increased the permanent deformation more than proportionally, indicating that the influence of stiffness modulus of the asphalt concrete was substantial and that the procedure recommended for stiffness estimation using the characteristics of the asphalt in the mix (11, 12), considered accurate within a factor of 2, requires careful evaluation for use in this part of the design process.

Figure 13 shows, at least for this set of circumstances [$h_1 = 12$ in. (30.5 cm)], that the subgrade stiffness had practically no effect on the accumulation of permanent deformation in the asphalt concrete layer. But, subgrade stiffness will influence the total permanent deformation at the pavement surface (a factor not considered in this analysis); and, for a given thickness, h_1 , total deformation will increase as the stiffness is reduced.

The influence of layer thickness on permanent deformation within the asphalt-bound layer is shown in Figure 14 to be minimal. This same result was reported by Hofstra and Klomp in their laboratory test track study. This comparison as well as those illustrated earlier indicates that the elastic theory for stress and strain distribution and a constitutive relationship determined from laboratory repeated load tests have the potential to assist in estimating permanent deformation accumulation in thick, asphalt-bound layers.

Viscoelastic Analysis

In this section the VESYS II procedure was used to examine the accumulation of permanent deformation in the same structure discussed in the previous section.

This procedure used a creep compliance determined from laboratory tests. Two conditions were used for compliance determination—compression and extension. Table 3 gives a summary of measured compliance values together with those determined from equations that were fit to the data. The 2 test techniques resulted in different compliance values, which, in turn, influenced rut depth prediction.

Results of the first part of the program are given in Table 4 and form the basis for subsequent calculations. Deflections computed from the data are shown in Figure 15 as a function of time for a 4,500-lb (20 000-N), single-wheel load with a contact pressure of 80 psi (550 kPa). In this system, the thickness of the asphalt layer (h_1) was taken as 12 in. (30.5 cm), and the subgrade modulus was assumed to be 5,000 psi (34 500 kPa).

In the portion of the program estimating the accumulation of permanent deformation, the time of loading (load assumed to vary with time as a Haversine function), t ,

Table 2. Factors used in deformation analysis.

| Temperature (F) | E ₁ (psi × 10 ⁶) | ν ₁ ^a | Coefficients of Equation 4 ^b | |
|-----------------|---|-----------------------------|---|------|
| | | | K | n |
| 72 | 1.0 | 0.21 | 0.22 | 0.62 |
| 85 | 0.51 | 0.28 | 0.32 | 0.66 |
| 100 | 0.225 | 0.36 | 0.44 | 0.70 |
| 114 | 0.1 | 0.43 | 0.56 | 0.73 |
| 126 | 0.05 | 0.50 | 0.63 | 0.76 |

Note: °C = 5/9 (°F - 32), 1 psi = 6.9 kPa.

^aν is a function of mixture stiffness or temperature or both.

^bDependent on temperature (see Fig. 6).

Figure 12. Influence of stiffness modulus on permanent deformation.

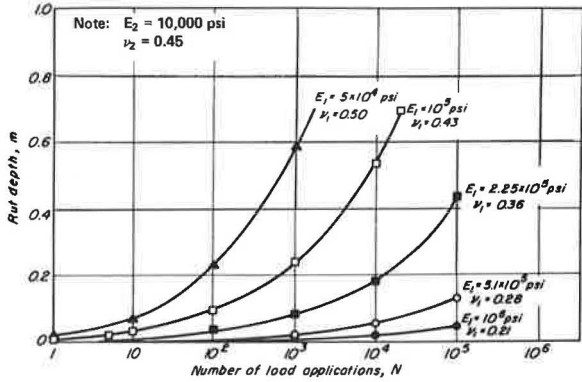


Figure 13. Influence of subgrade stiffness on permanent deformation.

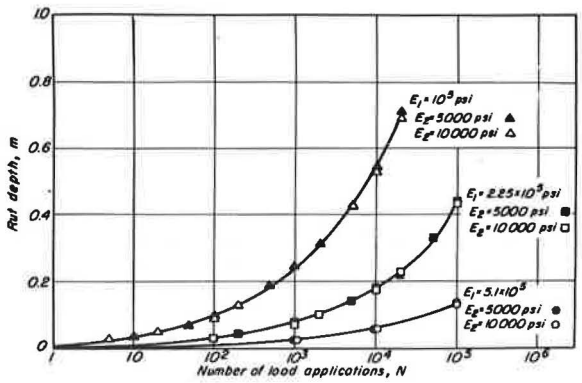


Figure 14. Influence of pavement thickness on permanent deformation.

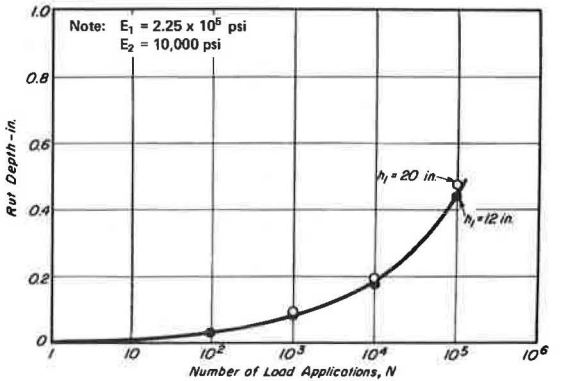


Table 3. Axial creep compliance values, measured and fitted.

| Time (sec) | Compression, 85 F | | Compression, 100 F | | Extension, 85 F | | Extension, 100 F | |
|------------|-----------------------|---------------------|-----------------------|---------------------|-----------------------|---------------------|-----------------------|---------------------|
| | Measured ^a | Fitted ^a | Measured ^a | Fitted ^a | Measured ^a | Fitted ^a | Measured ^a | Fitted ^a |
| 0.1 | 4.1 | 7.1 | 13.5 | 16.6 | 4.1 | 5.2 | 13.5 | 17.1 |
| 0.5 | | 11.0 | | 22.9 | | 9.4 | | 28.6 |
| 1.0 | 15.5 | 15.1 | 32.0 | 29.1 | 13.0 | 13.7 | 43.5 | 40.9 |
| 5.0 | | 29.2 | | 49.8 | | 31.2 | | 99.9 |
| 10 | 34.5 | 34.0 | 55.0 | 55.3 | 39.0 | 40.3 | 141.0 | 141.0 |
| 50 | | 45.3 | | 66.0 | | 70.1 | | 270.0 |
| 100 | 48.8 | 49.2 | 69.5 | 69.3 | 85.0 | 84.3 | 315.0 | 310.0 |
| 500 | | 59.1 | | 77.5 | | 124.0 | | 389.0 |
| 1,000 | 65.0 | 63.5 | 82.0 | 81.1 | 140.0 | 136.0 | 405.0 | 407.0 |
| 5,000 | | 78.3 | | 93.5 | | 183.0 | | 444.0 |
| 10,000 | 86.0 | 86.5 | 101.0 | 101.0 | 222.0 | 223.0 | 470.0 | 469.0 |
| 50,000 | | 109.0 | | 123.0 | | 341.0 | | 539.0 |
| 100,000 | | 112.0 | | 126.0 | | 358.0 | | 549.0 |

Note: °C = $\frac{5}{9}$ (°F - 32). Multiply compliance values by 0.145 to convert to 1/MPa.

^aThese values are in 10^{-6} in./in./psi.

Table 4. Axial creep compliance data, coefficients for Dirichlet series.

| δ_1 (1/sec) | $G_i \times 10^{-6}$ | | | |
|--------------------|----------------------|---------------------|------------------|-------------------|
| | Compression (85 F) | Compression (100 F) | Extension (85 F) | Extension (100 F) |
| 50 | 1.9 | -14.8 | -4.1 | -13.8 |
| 5.0 | -21.0 | -33.8 | -19.3 | -41.4 |
| 0.05 | -16.5 | -15.8 | -35.1 | -201.0 |
| 0.005 | -12.4 | -10.6 | -61.5 | -135.0 |
| 0.0005 | -14.3 | -10.1 | -14.6 | -24.9 |
| 0.00005 | -41.8 | -40.7 | -225.0 | -134.0 |
| 0 | 112.0 | 126.0 | 360.0 | 550.0 |

Note: Dirichlet series equation is $J(t) = \sum_{i=1}^n G_i \exp \delta_i t$.

°C = $\frac{5}{9}$ (°F - 32).

Figure 16. Computed permanent deformation versus number of load applications by using VESYS II; $t = 0.25$ sec, $T = 2.5$ sec.

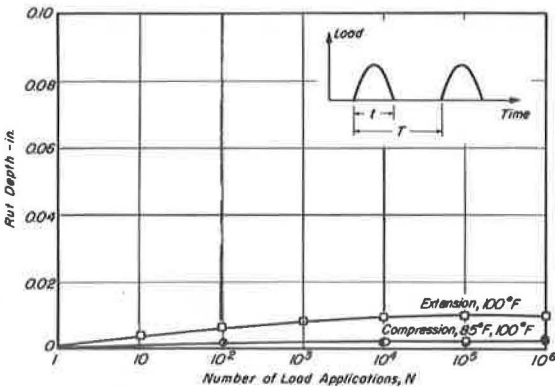


Figure 15. Computed deflection versus time.

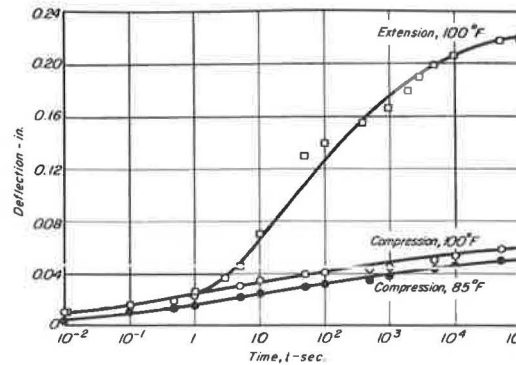
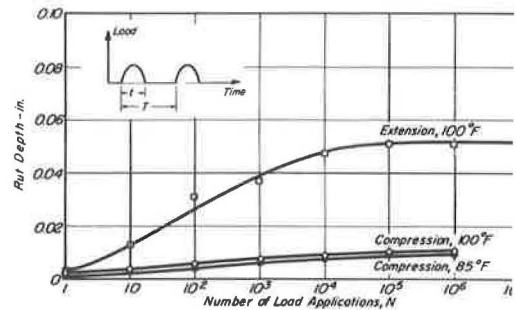


Figure 17. Computed permanent deformation versus number of load applications by using VESYS II; $t = 0.50$ sec, $T = 1.0$ sec.



and the total length of time before the next load is applied, T , are variables. Two conditions were used:

1. $t = 0.25$ sec, $T = 2.5$ sec (Fig. 16) and
2. $t = 0.50$ sec, $T = 1.0$ sec (Fig. 17).

In Figures 16 and 17, the permanent deformations that were estimated were substantially less than those computed earlier for essentially the same conditions. Moreover, the accumulation of permanent deformation with number of load applications by this procedure did not exhibit the same shape as that observed in the studies of Hofstra and Klomp. The reasons for these differences are not clear.

SUMMARY

Two procedures to predict permanent deformation in asphalt-bound layers by using laboratory-determined materials response were presented. One used repeated load triaxial compression tests and elastic theory; the other used a static creep test and viscoelastic theory.

Hofstra and Klomp presented data on rutting versus load repetitions under controlled conditions from studies on a laboratory test track. The repeated load test data and elastic theory provided the same form of relationship of rut depth versus load applications that was measured by Hofstra and Klomp. This suggests that the procedure can be used to examine this facet of the design problem. This approach, when used to study the influence of a number of parameters on pavement response, resulted in the following observations:

1. Subgrade stiffness appeared to have little influence on the accumulation of permanent deformation in the asphalt-bound layer—at least for the range in stiffnesses examined here;
2. Asphalt concrete stiffness exerted a significant influence on rutting in the asphalt-bound layer; and
3. Like the measurements of Hofstra and Klomp, the calculation procedure indicated that rut depth in the asphalt layer was independent of layer thickness for the range examined.

The creep test procedure estimated very little rutting. Moreover, the shape of the rut depth versus the application relationship determined by this methodology did not resemble the form reported by Hofstra and Klomp. These observations indicate that a careful evaluation must be made of this procedure to ascertain the reasons for these discrepancies.

In the judgment of the authors, neither of the methods is suitable for present design implementation.

ACKNOWLEDGMENTS

The authors wish to acknowledge the support provided by the staff and facilities of the Institute of Transportation and Traffic Engineering, University of California, Berkeley. The investigation was supported in part by the Transportation Laboratory of the California Department of Transportation and the Federal Highway Administration. Neither agency has reviewed the findings.

REFERENCES

1. Heukelom, W., and Klomp, A. J. G. Consideration of Calculated Strains at Various Depths in Connection With the Stability of Asphalt Pavements. Proc. Second Internat. Conf. on Structural Design of Asphalt Pavements, Univ. of Michigan, Ann Arbor, 1967.
2. Barksdale, R. D. Laboratory Evaluation of Rutting in Base Course Materials. Proc. Third Internat. Conf. on Structural Design of Asphalt Pavements, Univ. of Michigan, Ann Arbor, 1972.
3. Romain, J. E. Rut Depth Prediction in Asphalt Pavements. Proc. Third Internat. Conf. on Structural Design of Asphalt Pavements, Univ. of Michigan, Ann Arbor, 1972.

4. Elliott, J. F., and Moavenzadeh, F. Moving Load on Viscoelastic Layered System, Phase II. Dept. of Civil Engineering, Massachusetts Institute of Technology, Cambridge, Mass., Rept. R69-64, Sept. 1969.
5. Elliott, J. F., Moavenzadeh, F., and Findakly, H. Moving Load on Viscoelastic Layered Systems, Phase II—Addendum. Dept. of Civil Engineering, Massachusetts Institute of Technology, Cambridge, Mass., Res. Rept. R70-20, April 1970.
6. Hofstra, A., and Klomp, A. J. G. Permanent Deformation of Flexible Pavements Under Simulated Road Traffic Conditions. Proc. Third Internat. Conf. on Structural Design of Asphalt Pavements, Univ. of Michigan, Ann Arbor, 1972.
7. McLean, D. B. Permanent Deformation Characteristics of Asphalt Concrete. Univ. of California, Berkeley, PhD dissertation, 1974.
8. Dehlen, G. L. The Effect of Non-Linear Material Response on the Behavior of Pavements Subjected to Traffic Loads. Univ. of California, Berkeley, PhD dissertation, 1969.
9. Kenis, W. J., and McMahan, T. F. Advance Notice of FHWA Pavement Design System and a Design Check Procedure. Presented at AASHO Design Committee Meeting, Oct. 1972.
10. Mendelson, A. Plasticity: Theory and Practice. Macmillan Publishing Co., Riverside, N. J., 1968.
11. Van der Poel, C. A General System Describing the Viscoelastic Properties of Bitumens and Its Relation to Routine Test Data. Jour. Appl. Chem., Vol. 4, Part 5, May 1954, pp. 221-236.
12. Heukelom, W., and Klomp, A. J. G. Road Design and Dynamic Loadings. Proc. Assoc. of Asphalt Paving Technologists, Minneapolis, Vol. 33, 1964, pp. 92-125.

APPENDIX

TRIAXIAL COMPRESSION TEST PROGRAM

Loading Conditions

In this investigation the pavement was represented as a multilayer elastic system in which the material properties were varied to reflect their nonlinear response characteristics. The magnitudes of applied stresses that resulted from loads applied to dual tires lie within the shaded areas shown in Figure 18. Examination of varying stress at varying distances from a point provided an indication of the shape of the stress-time curve to be used. Recommended shapes are given in Table 5. Also included in this table are suggestions for the stress conditions to be utilized. Time of loading, t , data that are shown in Figure 19 and referenced in Table 5 indicate that the horizontal stress was usually longer than the vertical. This might exert a substantial influence on the deformation characteristics of asphalt concrete.

Equipment

The triaxial compression test system used in this phase of the investigation was developed by Dehlen (8). In this system the axial and radial stresses can be independently applied. This independence, as shown in Figure 21, was obtained by loading the specimen axially from the bottom with a loading area equal to that of the specimen; a Bellofram was used to seal the axial loading piston. Axial compression or tension was applied by a double-acting 4-in.- (10.2-cm-) diameter Bellofram piston. Radial pressure was obtained by filling the chamber with silicone oil and by applying air pressure to it through a Bellofram piston interface.

A pneumatic timer control unit was developed for the system consisting of 4 pneumatic elements. Figure 22 shows how it functioned. Two elements were activated at the start of the cycle and provided signals of duration t_1 and t_2 . Signal t_1 was the "on-time" signal to either the axial or radial loading system. Signal t_2 introduced a delay before the third element was activated. This element provided an "on" signal of

Figure 18. Probable ranges of stress combinations in layer combinations in layer 1 (asphalt layer) of a 2-layer system.

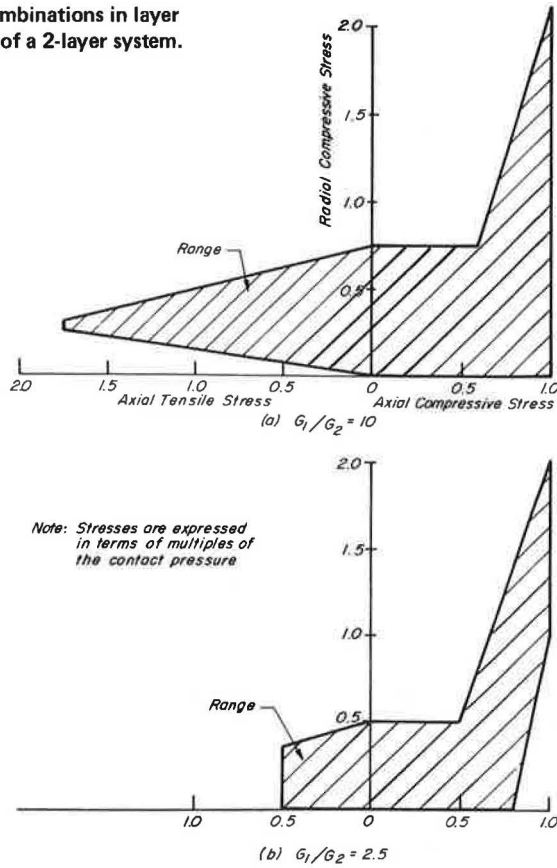


Table 5. Summary of stress-time conditions.

| Location and Stress Direction | Shape of Stress-Time Curve | Horizontal-Vertical t Ratio | Horizontal-Vertical Stress Ratio |
|-------------------------------|----------------------------|-----------------------------|--|
| Near surface | | | |
| Vertical | Square | See Figure 19 | Less than 1 $< \frac{\sigma_v}{\sigma_h} < 5.0$ |
| Horizontal | Triangle | See Figure 19 | Less than 1 $< \frac{\sigma_v}{\sigma_h} < 5.0$ |
| Intermediate depth | | | |
| Vertical | Triangle | See Figure 19 | Horizontal stresses may be zero, tensile, or compressive |
| Horizontal | Triangle | See Figure 19 | Horizontal stresses may be zero, tensile, or compressive |
| Bottom | | | |
| Vertical | Triangle | 1.0 | See Figure 20 |
| Horizontal | Triangle | 1.0 | See Figure 20 |

Figure 19. Horizontal-vertical t ratio, range in modular ratios.

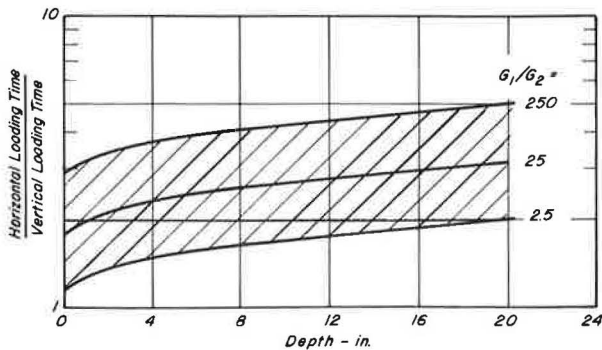


Figure 20. Horizontal-vertical stress ratio at the base of layer 1 versus modular ratio of the 2 layers.

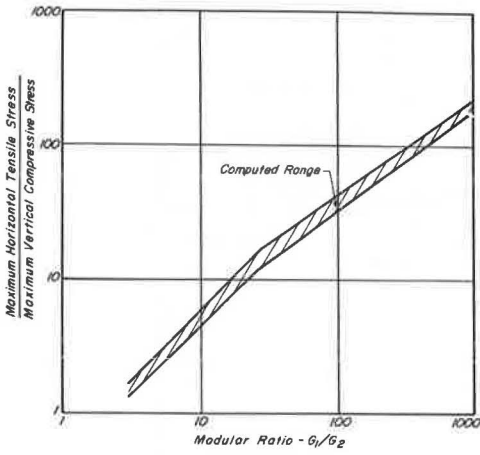


Figure 21. Triaxial apparatus that permits independent variation of axial and radial stresses.

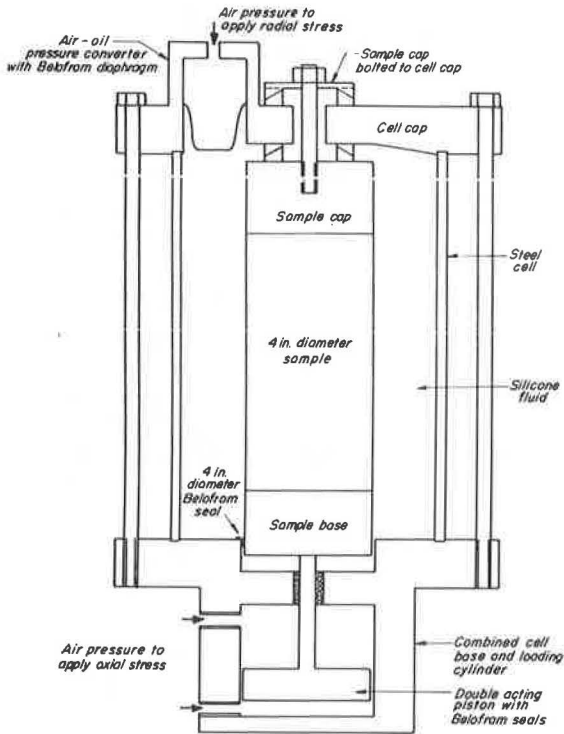


Figure 22. Timer signal outputs.

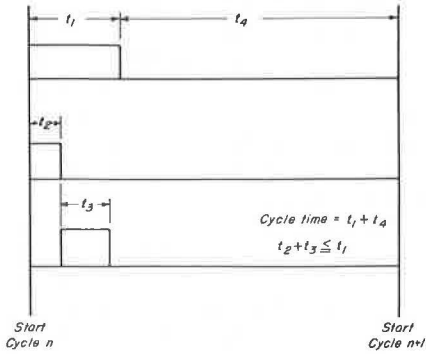


Figure 23. Triaxial loading system for repetitive loading tests.

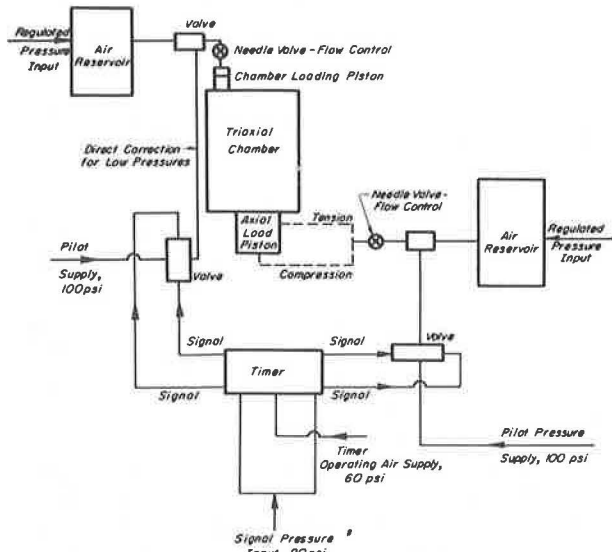
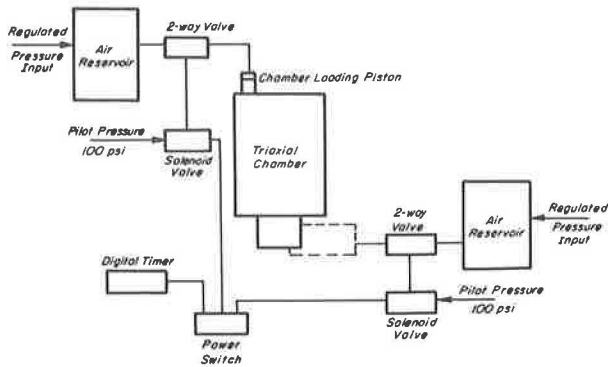


Figure 24. Triaxial loading system for creep tests.



duration t_3 to the second loading element. The fourth timer element controlled the off-load of the system. Times t_1 to t_4 were adjustable from zero to 30 sec.

Output signals from the timer involved only a small line flow of air, insufficient to operate large air valves. Therefore, a booster system was required as shown in Figure 23. By using this approach and maintaining short flow distances from air reservoirs to the loading pistons, rise times (time from zero to full load) could be reduced to 0.007 sec. When longer load rise times were required, needle valves were introduced to control the air flow rates. Because of limitations imposed by valve response times, the minimum load duration that could be obtained was 0.035 sec.

This equipment also was used for creep tests. For these tests the timer portion of the repetitive loading system was replaced by a digital clock reading to 0.01 min. The main air valves were operated by using electric solenoid valves. A main switch activated the solenoid valves and timer simultaneously. System components are shown in Figure 24. Use of high air pilot pressures resulted in rapid valve response times with the result that load rise times were less than 0.01 sec in all tests. Loading times of less than 1 min were measured by using the timer portion of the Sanborn recorder system. Times greater than 1 min were established from the digital clock.

Deformations in the specimens were measured by using linear variable differential transformers firmly attached to the specimens.

Procedures

Repeated Loading—The 3 loading conditions studied in the laboratory were chosen because the pneumatic loading equipment could not completely simulate actual conditions. These were

1. Horizontal compression midway between the loaded areas (by extension tests);
2. Horizontal stress near the point of zero (by unconfined compression tests); and
3. Axial tension and radial compression with the same loading time at the base of the layer (by tension tests).

Because of the time-dependent recovery properties of asphalt concrete, the amount of permanent deformation was expected to depend on the time interval between load applications. In preliminary tests deformation recovery approached zero at a cycle time of 6 sec. This value was selected for use in the study.

Creep Loading—Prior conditioning influenced the response of asphalt concrete in creep loading. In this study the procedure that finally was adopted included the application of a larger stress than that to be used in test for a period of 10 min followed by 2 repetitions of the desired stress applied for a period of 15 min. Recovery times of 1 to 1.5 hours were allowed between each load application. Deformations from the second or third application were used to compute compliance relationships. The 2 loading conditions were unconfined axial compression and axial extension.